

1 **Ecophysiology of freshwater Verrucomicrobia inferred from genomes**  
2 **recovered through time-series metagenomics**

3  
4 Shaomei He<sup>1,2</sup>, Sarah LR Stevens<sup>1</sup>, Leong-Keat Chan<sup>4</sup>, Stefan Bertilsson<sup>3</sup>, Tijana Glavina del  
5 Rio<sup>4</sup>, Susannah G Tringe<sup>4</sup>, Rex R Malmstrom<sup>4</sup>, and Katherine D McMahon<sup>1,5,\*</sup>

6  
7 <sup>1</sup>Department of Bacteriology, University of Wisconsin-Madison, Madison, WI, USA

8 <sup>2</sup>Department of Geoscience, University of Wisconsin-Madison, Madison, WI, USA

9 <sup>3</sup>Department of Ecology and Genetics, Limnology and Science for Life Laboratory, Uppsala  
10 University, Uppsala, Sweden

11 <sup>4</sup>DOE Joint Genome Institute, Walnut Creek, CA, USA

12 <sup>5</sup>Department of Civil and Environmental Engineering, University of Wisconsin-Madison,  
13 Madison, WI, USA

14

15 **\*Corresponding author**

16 Katherine D McMahon

17 1550 Linden Drive

18 5552 Microbial Sciences Building

19 Madison, WI 53706, USA

20 [trina.mcmahon@wisc.edu](mailto:trina.mcmahon@wisc.edu)

21

22

23 **Running title:** Freshwater Verrucomicrobia ecophysiology inferred from genomics

24

25 **Keywords:** Metagenome-assembled genome (MAG), Verrucomicrobia, Freshwater,  
26 Glycoside hydrolase, Nutrient limitation, Cytochrome *c*

27

28 **ABSTRACT**

29 Microbes are critical in carbon and nutrient cycling in freshwater ecosystems. Members of  
30 the Verrucomicrobia are ubiquitous in such systems, yet their roles and ecophysiology are  
31 not well understood. In this study, we recovered 19 Verrucomicrobia draft genomes by  
32 sequencing 184 time-series metagenomes from a eutrophic lake and a humic bog that differ  
33 in carbon source and nutrient availabilities. These genomes span four of the seven  
34 previously defined Verrucomicrobia subdivisions, and greatly expand the known genomic  
35 diversity of this freshwater lineage. Genome analysis revealed their role as  
36 (poly)saccharide-degraders in freshwater, uncovered interesting genomic features for this  
37 life style, and suggested their adaptation to nutrient availabilities in their environments.  
38 Between the two lakes, Verrucomicrobia populations differ significantly in glycoside  
39 hydrolase gene abundance and functional profiles, reflecting the autochthonous and  
40 terrestrially-derived allochthonous carbon sources of the two ecosystems respectively.  
41 Several bog populations exhibited nitrogen cost minimization in their proteomes and  
42 genomes, which is likely an adaptation to long-term nitrogen limitation in the bog.  
43 Interestingly, a number of genomes recovered from the bog contained gene clusters that  
44 potentially encode a novel porin-multiheme cytochrome *c* complex and might be involved  
45 in extracellular electron transfer in the anoxic humic-rich environment. Notably, most  
46 epilimnion genomes have large numbers of Planctomycete-specific cytochrome *c*-  
47 containing genes, which exhibited nearly opposite distribution patterns with glycoside  
48 hydrolase genes, probably associated with the different environmental oxygen availability  
49 and carbohydrate complexity between lakes/layers. Overall, the recovered genomes are a  
50 major step towards understanding the role, ecophysiology and distribution of  
51 Verrucomicrobia in freshwater.

52

## 53 INTRODUCTION

54 Microbes play important roles in mediating carbon (C) and nutrient cycling in freshwater  
55 ecosystems. Among them are the ubiquitous Verrucomicrobia, which exhibit a  
56 cosmopolitan distribution in freshwater lakes. For example, they were present in 90% of  
57 81 studied lakes (Zwart et al 2003). Verrucomicrobia abundances often range between  
58 <1% to 6% of the total microbial community (Eiler and Bertilsson 2004, Newton et al 2011,  
59 Parveen et al 2013), and contributed up to 19% in a humic lake (Arnds et al 2010). Yet, in  
60 comparison to other freshwater bacterial groups, such as members of the Actinobacteria,  
61 Cyanobacteria and Proteobacteria phyla, Verrucomicrobia have received relatively less  
62 attention, and their functions and ecophysiology in freshwater are not well understood.

63 As a phylum, Verrucomicrobia (V) was first proposed relatively recently, in 1997  
64 (Hedlund et al 1997). Together with Planctomycetes (P), Chlamydiae (C), and sister phyla  
65 such as Lentisphaerae, they comprise the PVC superphylum. In addition to being  
66 cosmopolitan in freshwater, Verrucomicrobia have been found in oceans (Yoon et al 2007,  
67 Yoon et al 2008), soil (Sangwan et al 2005), wetlands (Qiu et al 2014), rhizosphere (da  
68 Rocha et al 2010), and animal guts (Derrien et al 2004, Wertz et al 2012), as free-living  
69 organisms or symbionts of eukaryotes. Verrucomicrobia isolates are metabolically diverse,  
70 including aerobes, facultative anaerobes, and obligate anaerobes, and they are mostly  
71 heterotrophs, using various mono-, oligo-, and poly-saccharides for growth (Chin et al  
72 2001, Derrien et al 2004, Hedlund et al 1996, Hedlund et al 1997, Otsuka et al 2013a,  
73 Otsuka et al 2013b, Qiu et al 2014, Sangwan et al 2004, Scheuermayer et al 2006, Yoon et al  
74 2007). Not long ago an autotrophic verrucomicrobial methanotroph (*Methylacidiphilum*

75 *fumariolicum* SolV) was discovered in acidic thermophilic environments as the only non-  
76 proteobacterial aerobic methanotroph to date (Pol et al 2007).

77 In marine environments, Verrucomicrobia are also ubiquitous (Freitas et al 2012)  
78 and suggested to have a key role as polysaccharide degraders (Cardman et al 2014,  
79 Martinez-Garcia et al 2012a). Genomic insights gained through sequencing single cells  
80 (Martinez-Garcia et al 2012a) or extracting Verrucomicrobia bins from metagenomes  
81 (Herlemann et al 2013) have revealed high abundances of glycoside hydrolase genes,  
82 providing more evidence for their critical roles in C cycling in marine environments.

83 In freshwater, Verrucomicrobia have been suggested to degrade glycolate (Paver  
84 and Kent 2010) and polysaccharides (Martinez-Garcia et al 2012a). The abundance of  
85 some phylum members was favored by high nutrient availabilities (Haukka et al 2006,  
86 Lindström et al 2004), algal blooms (Kolmonen et al 2004), low pH, high temperature, high  
87 hydraulic retention time (Lindström et al 2005), and more labile DOC (Arnds et al 2010).  
88 To date, there are very few freshwater Verrucomicrobia isolates, including  
89 *Verrucomicrobium spinosum* (Schlesner 1987) and several *Prostheco bacter* spp. (Hedlund  
90 et al 1997). Physiological studies showed that they are aerobes, primarily using  
91 carbohydrates, but not amino acids, alcohols, or rarely organic acids for growth. However,  
92 these few cultured isolates only represent a single clade within subdivision 1. By contrast,  
93 16S rRNA gene based studies discovered a much wider phylogenetic range of freshwater  
94 Verrucomicrobia, including subdivisions 1, 2, 3, 4, 5, and 6 (Arnds et al 2010, Eiler and  
95 Bertilsson 2004, Martinez-Garcia et al 2012a, Parveen et al 2013, Zwart et al 1998). Due to  
96 the very few cultured representatives and few available genomes from this freshwater

97 lineage, the ecological functions of the vast uncultured freshwater Verrucomicrobia are  
98 largely unknown.

99 In this study, we sequenced a total of 184 metagenomes in a time-series study of two lakes  
100 with contrasting characteristics, particularly differing in C source, nutrient availabilities,  
101 and pH. We recovered a total of 19 Verrucomicrobia draft genomes spanning subdivision 1,  
102 2, 3, and 4 of the seven previously defined Verrucomicrobia subdivisions. We inferred their  
103 metabolisms, revealed their adaptation to C and nutrient conditions, and uncovered some  
104 interesting and novel features, including a novel putative porin-multiheme cytochrome  
105 system that may be involved in extracellular electron transfer. The gained insights  
106 advanced our understanding of the ecophysiology, roles in C cycling, and ecological niches  
107 of this ubiquitous freshwater bacterial group.

108

## 109 **MATERIALS AND METHODs**

110 **Study sites.** Samples for metagenome sequencing were collected from two temperate lakes  
111 in Wisconsin, USA, Lake Mendota and Trout Bog Lake, during ice-off periods of each year  
112 (May to November). Mendota is an urban eutrophic lake with most of its C being  
113 autochthonous (in-lake produced), whereas Trout Bog is a small, acidic and nutrient-poor  
114 dystrophic lake with mostly terrestrially-derived (allochthonous) C. General lake  
115 characteristics are summarized in **Table 1**.

116

117 **Sampling.** For Mendota, we collected depth-integrated water samples from the surface 12  
118 m (mostly consisting of the epilimnion layer) at 94 time points from 2008 to 2012, and  
119 samples were referred to as “ME” (Garcia et al 2016). For Trout Bog, we collected the

120 integrated hypolimnion layer at 45 time points from 2007 to 2009 and the integrated  
121 epilimnion layer at 45 time points from 2007 to 2009, and samples were referred to as  
122 “TH” and “TE”, respectively (Bendall et al 2016). All samples were filtered through 0.22  $\mu$   
123 m polyethersulfone filters and stored at -80°C until extraction. DNA was extracted from the  
124 filters using the FastDNA kit (MP Biomedicals) according to manufacturer’s instruction  
125 with some minor modifications as described previously (Shade et al 2008).

126

127 **Metagenome sequencing, assembly, and draft genome recovery.** Details of  
128 metagenome sequencing, assembly, and binning were described in Bendall *et al.* (2016)  
129 and Hamilton et al (preprint). Briefly, shotgun Illumina HiSeq 2500 metagenome libraries  
130 were constructed for each of the DNA samples. Three combined assemblies were generated  
131 by co-assembling reads from all metagenomes within the ME, TE, and TH groups,  
132 respectively. Binning was conducted on the three combined assemblies to recover  
133 “metagenome-assembled genomes” (MAGs) based on the combination of contig  
134 tetranucleotide frequency and differential coverage patterns across time points using  
135 MetaBAT (Kang et al 2015). Subsequent manual curation of MAGs was conducted to  
136 remove contigs that did not correlate well with the median temporal abundance pattern of  
137 all contigs within a MAG, as described in Bendall *et al.* (2016).

138

139 **Genome annotation and completeness estimation.** MAGs were submitted to the DOE  
140 Joint Genome Institute’s Integrated Microbial Genome (IMG) database for gene prediction  
141 and function annotation (Markowitz et al 2013). The IMG Taxon Object IDs for  
142 Verrucomicrobia MAGs are listed in **Table 2**. The completeness of each MAG was estimated

143 based on the number of recovered single-copy essential genes compared to the total of 105  
144 single-copy essential genes expected for complete Verrucomicrobia genomes (Albertsen et  
145 al 2013). MAGs with an estimated completeness lower than 50% were not included in this  
146 study.

147

148 **Taxonomic and phylogenetic analysis.** A total of 19 MAGs were classified to the  
149 Verrucomicrobia phylum based on taxonomic assignment by PhyloSift using 37 conserved  
150 phylogenetic marker genes (Darling et al 2014), as described in Bendall *et al.* (2016). A  
151 phylogenetic tree was reconstructed from the 19 Verrucomicrobia MAGs and 24 reference  
152 genomes using an alignment concatenated from individual protein alignments of five  
153 conserved essential single-copy genes (represented by TIGR01391, TIGR01011,  
154 TIGR00663, TIGR00460, and TIGR00362) that were recovered in all Verrucomicrobia  
155 MAGs. Individual alignments were first generated with MUSCLE (Edgar 2004),  
156 concatenated, and trimmed to exclude columns that contain gaps for more than 30% of all  
157 sequences. A maximum likelihood phylogenetic tree was constructed using PhyML 3.0  
158 (Guindon et al 2010), with the LG substitution model and the gamma distribution  
159 parameter estimated by PhyML. Bootstrap values were calculated based on 100 replicates.  
160 *Kiritimatiella glycovorans* L21-Fru-AB was used as an outgroup in the phylogenetic tree.  
161 This bacterium was initially designated as the first (and so far the only) cultured  
162 representative of Verrucomicrobia subdivision 5. However, this subdivision was later  
163 proposed as a novel sister phylum associated with Verrucomicrobia (Spring et al 2016),  
164 making it an ideal outgroup for this analysis.

165

166 **Estimate of metabolic potential.** IMG provides functional annotation based on KO (KEGG  
167 orthology) term, COG (cluster of orthologous group), pfam, and TIGRfam. To estimate  
168 metabolic potential, we primarily used KO terms due to their direct link to KEGG pathways.  
169 COG, pfam, and TIGRfam were also used when KO terms are not available for a function.  
170 Pathways are primarily reconstructed according to KEGG modules, and MetaCyc pathway is  
171 used if a KEGG module is not available for a pathway. As these MAGs are incomplete  
172 genomes, a fraction of genes in a pathway may be missing due to genome incompleteness.  
173 Therefore, we estimated the completeness of a pathway as the fraction of recovered  
174 enzymes in that pathway (e.g. a pathway is 100% complete if all enzymes in that pathway  
175 are encoded by genes recovered in a MAG). As some genes are shared by multiple  
176 pathways, signature genes specific for a pathway were used to indicate the presence of a  
177 pathway. If signature genes for a pathway were missing in all MAGs, that pathway was  
178 likely absent in all genomes. Based on this, we established criteria for estimating pathway  
179 completeness in each MAG. If a signature gene in a pathway was present, we report the  
180 percentage of genes in the pathway that we found. If a signature gene was absent in a MAG,  
181 but present in at least one third of all MAGs (i.e.  $\geq 7$ ), we still report the pathway  
182 completeness for that MAG in order to account for genome incompleteness. Otherwise, we  
183 considered the pathway to be absent (i.e. completeness is 0%).

184

185 **Glycoside hydrolase identification.** Glycoside hydrolase (GH) genes were identified using  
186 the dbCAN annotation tool (<http://csbl.bmb.uga.edu/dbCAN/annotate.php>) (Yin et al  
187 2012) using HMMER search against hidden Markov models (HMMs) built for all GHs, with  
188 an E-value cutoff of  $1e-7$ , except GH109, for which we found that the HMM used by dbCAN



189 is not specific for this GH. To identify verrucomicrobial GH109, BLASTP was performed  
190 using GH109 sequences from verrucomicrobial *Akkermansia muciniphila* ATCC BAA-835  
191 listed in the CAZy database (<http://www.cazy.org>), with E-value cutoff of 1e-6 and query  
192 sequence coverage cutoff of 50%.

193  
194 **Other bioinformatic analyses.** Protein cellular location was predicted using CELLO v.2.5  
195 (<http://cello.life.nctu.edu.tw>) (Yu et al 2006) and PSORTb v.3.0  
196 (<http://www.psорт.org/psортb>) (Yu et al 2010). The beta-barrel structure of outer  
197 membrane proteins was predicted by PRED-TMBB  
198 (<http://bioinformatics.biol.uoa.gr//PRED-TMBB>) (Bagos et al 2004).

199

## 200 **RESULTS AND DISCUSSION**

### 201 **Comparison of the two lakes**

202 The two studied lakes exhibited contrasting characteristics (**Table 1**). The most notable  
203 difference is the primary C source and nutrient availabilities. Mendota is an urban  
204 eutrophic lake with most of its C being autochthonous (in-lake produced through  
205 photosynthesis). By contrast, Trout Bog is a nutrient-poor dystrophic lake, surrounded by  
206 boreal forests and sphagnum mats, thus receiving large amounts of terrestrially-derived  
207 allochthonous C that is rich in humic and fulvic acids. Compared to Mendota, Trout Bog  
208 features higher DOC levels, but is more limited in nutrient availability, with much higher  
209 DOC:TN and DOC:TP ratios (**Table 1**). Nutrient limitation in Trout Bog is even more  
210 extreme than revealed by these ratios because much of the N and P is tied up in complex  
211 dissolved organic matter. In addition, Trout Bog has lower oxygenic photosynthesis due to

212 decreased photosynthetically active radiation (PAR) as a result of absorption by DOC (Read  
213 and Rose 2013). Together with the high consumption of dissolved oxygen by heterotrophic  
214 respiration, oxygen levels decrease quickly with depth in the water column in Trout Bog.  
215 Dissolved oxygen levels are below detection in the hypolimnion nearly year-round (Shade  
216 et al 2008). Due to these contrasts, we expected to observe differences in bacterial C and  
217 nutrient use, as well as differences reflecting the electron acceptor conditions between  
218 these two lakes. Hence, the retrieval of numerous Verrucomicrobia draft genomes in the  
219 two lakes not only allows the revelation of their general functions in freshwater, but also  
220 provides an opportunity to study their ecophysiological adaptation associated with the  
221 local environmental differences.

222

### 223 **Verrucomicrobia draft genome retrieval and their distribution patterns**

224 Using the binning facilitated by tetranucleotide frequency and relative abundance patterns  
225 over time, a total of 19 Verrucomicrobia MAGs were obtained, including eight from ME,  
226 three from TE, and eight from TH (**Table 2**). The 19 MAGs exhibited a clustering of their  
227 tetranucleotide frequency largely based on the two lakes (**Figure S1**), suggesting distinct  
228 overall genomic signatures associated with each system.

229 Genome completeness of the 19 MAGs ranged from 53% to 96%, as determined  
230 based on the 105 single-copy essential genes expected for complete Verrucomicrobia  
231 genomes (Albertsen et al 2013). We performed phylogenetic analysis of these MAGs using a  
232 concatenated alignment of their conserved genes, and found that they span a wide  
233 phylogenetic spectrum and distribute in subdivisions 1, 2, 3, and 4 of the seven previously  
234 defined Verrucomicrobia subdivisions (Arnds et al 2010, Pol et al 2007, Schlesner et al

235 2006) (**Figure 1**), as well as three unclassified Verrucomicrobia MAGs. In fact, the  
236 phylogenetic diversity of Verrucomicrobia in these two lakes is higher than that  
237 represented by these 19 MAGs. For example, an un-binned contig from the Mendota  
238 metagenome is likely from subdivision 6 representing the freshwater clade LD19 (Zwart et  
239 al 2003), as its genes share an average amino acid identity of 89% with previously  
240 recovered MAGs from subdivision 6 (Hugerth et al 2015). Notably, this contig contains a  
241 gene encoding proteorhodopsin, a light-driven proton pump, consistent with a previously  
242 recovered rhodopsin gene from a freshwater Verrucomicrobia single cell genome  
243 (Martinez-Garcia et al 2012b). However, no rhodopsin gene was observed in any of the 19  
244 other higher quality Verrucomicrobia MAGs that were analyzed extensively in this study.  
245 Nevertheless, we restricted our analysis to the 19 MAGs based on their high quality, while  
246 at the same time acknowledging that they do not cover all the genomic diversity of  
247 Verrucomicrobia populations in our study systems.

248 Presently available freshwater Verrucomicrobia isolates are restricted to  
249 subdivision 1. The recovered MAGs allow the inference of metabolisms and ecology of a  
250 considerable diversity within uncultured freshwater Verrucomicrobia. Notably, all MAGs  
251 from subdivision 3 were recovered from TH, and all MAGs from subdivision 1, except  
252 TH2746, were from the epilimnion (either ME or TE), indicating differences in phylogenetic  
253 distribution between lakes and between layers within a lake.

254 We used normalized fold coverage of MAGs within individual metagenomes to  
255 comparatively infer relative population abundance (see detailed coverage depth estimation  
256 in **Supplementary Text**). Briefly, we counted the number of reads mapping with a  
257 minimum identity of 95% and calculated a relative abundance for each MAG based on

258 coverage depth per contig and several normalization steps. Thus, we assume that each  
259 MAG represents a distinct population within the lake-layer from which it was recovered  
260 (Bendall et al 2016, Garcia et al 2016). This estimate does not directly indicate the actual  
261 relative abundance of these populations within the total community per se; rather it allows  
262 us to compare population abundance levels from different lakes and sampling occasions  
263 within the set of 19 MAGs. This analysis indicates that Verrucomicrobia populations in  
264 Trout Bog were proportionally more abundant and persistent over time compared to those  
265 in Mendota (**Figure 2**). Verrucomicrobia populations in Mendota were only transiently  
266 abundant, bloomed once to a few times during the sampling season and diminished to  
267 extremely low levels for the remainder of the year.

268

### 269 **Saccharolytic life style and adaptation to different C sources**

270 Verrucomicrobia isolates from different environments are known to grow on various  
271 mono-, oligo-, and poly-saccharides, but are unable to grow on amino acids, alcohols, or  
272 most organic acids (Chin et al 2001, Derrien et al 2004, Hedlund et al 1996, Hedlund et al  
273 1997, Otsuka et al 2013a, Otsuka et al 2013b, Qiu et al 2014, Sangwan et al 2004,  
274 Scheuermayer et al 2006, Shieh and Jean 1998, Yoon et al 2007). Culture-independent  
275 research suggests marine Verrucomicrobia as candidate polysaccharide degraders with  
276 large number of genes involved in polysaccharide utilization (Cardman et al 2014,  
277 Herlemann et al 2013, Martinez-Garcia et al 2012a).

278 In the 19 Verrucomicrobia MAGs, we observed rich arrays of glycoside hydrolase  
279 (GH) genes, representing a total of 78 different GH families acting on diverse  
280 polysaccharides (**Figure S2**). As these genomes have different degrees of completeness, to

281 compare among them, we normalized GH occurrence frequencies by the total number of  
282 genes in each MAG to estimate the percentage of genes annotated as GHs (i.e. GH coding  
283 density), which ranged from 0.4% to 4.9% for these MAGs (**Figure 3a**). In general, GH  
284 coding density was higher in Trout Bog MAGs than in Mendota MAGs. Notably, six TH MAGs  
285 had extremely high (~4%) GH coding densities (**Figure 3a**), with each MAG harboring 119-  
286 239 GH genes, representing 36-59 different GH families (**Figures 4 & S2**). Although GH  
287 coding density in most ME genomes in subdivisions 1 and 2 was relatively low (0.4-1.6%),  
288 it was still higher than in many other bacterial groups (Martinez-Garcia et al 2012a).

289         The GH abundance and diversity within a genome may determine the width of the  
290 substrate spectrum and/or the complexity of carbohydrates used by that organism. For  
291 example, there are 20 GH genes in the *Rubritalea marina* genome, and this marine  
292 verrucomicrobial aerobe only uses a limited spectrum of carbohydrate monomers and  
293 dimers, but not the majority of (poly)saccharides tested (Scheuermayer et al 2006). By  
294 contrast, 164 GH genes are present in the *Opitutus terrae* genome, and this soil  
295 verrucomicrobial anaerobe can thus grow on a wider range of mono-, di- and poly-  
296 saccharides (Chin et al 2001). Therefore, it is plausible that the GH-rich Trout Bog  
297 Verrucomicrobia populations may be able to use a wider range of more complex  
298 polysaccharides than the Mendota populations.

299         The 10 most abundant GH families in these Verrucomicrobia MAGs include GH2, 29,  
300 78, 95, and 106 (**Figure 4**). These specific GHs were absent or at very low abundances in  
301 marine Verrucomicrobia genomes (Herlemann et al 2013, Martinez-Garcia et al 2012a),  
302 suggesting a general difference in carbohydrate substrate use between freshwater- and  
303 marine Verrucomicrobia. Hierarchical clustering of MAGs based on overall GH abundance

304 profiles indicated a grouping pattern largely separated by lake (**Figure S3**). Prominently  
305 over-represented GHs in most Trout Bog MAGs include GH29, 78, 95, and 106, all of which  
306 mainly function as  $\alpha$ -L-fucosidases or  $\alpha$ -L-rhamnosidases, as well as GH2, a  $\beta$ -  
307 galactosidase that also acts on other  $\beta$ -linked dimers. By contrast, over-represented GHs  
308 in the Mendota MAGs are GH13, 20, 33, 57, and 77. Among them, GH13 and 57 are  $\alpha$ -  
309 amylases, and GH20 is  $\beta$ -hexosaminidases, clearly exhibiting different substrate spectra  
310 from GHs over-represented in the Trout Bog MAGs. Therefore, the patterns in GH  
311 functional profiles may suggest varied carbohydrate substrate preferences and ecological  
312 niches occupied by Verrucomicrobia, probably reflecting the different carbohydrate  
313 composition derived from different sources between Mendota and Trout Bog.

314 A particularly interesting contrast of GH genes was observed between ME3880 and  
315 TH2746. These two populations were phylogenetically close relatives in subdivision 1  
316 (**Figure 1**), and had an average nucleotide identity of 74% among the 654 bi-directional  
317 best hits between the two genomes. Albeit that, their estimated genome sizes differ  
318 substantially (**Table 2**). Notably, TH2746 possesses a total of 239 GH genes, whereas  
319 ME3880 has only 17 GH genes, despite the two MAGs having comparably high levels of  
320 completeness. Based on the GH diversity and abundance profile (**Figures 3a, 4, and S3**),  
321 TH2746 is an outlier of subdivision 1, and instead shares more similarity to other TH  
322 genomes in subdivision 3. Therefore this subdivision 1 Verrucomicrobia population  
323 genome might have been expanded to adapt to the carbohydrate substrate composition in  
324 Trout Bog.

325 Overall, GH diversity and abundance profile may reflect the DOC availability,  
326 chemical variety and complexity, and may suggest microbial adaptation to different C

327 sources in the two ecosystems. We speculate that the rich arrays of GH genes, and  
328 presumably broader substrate spectra of Trout Bog populations, partly contribute to their  
329 higher abundance and persistence over the sampling season (**Figure 2**), as they are less  
330 likely impacted by fluctuations of individual carbohydrates; whereas Mendota populations  
331 with fewer GHs and presumably more specific substrate spectra are relying on  
332 autochthonous C and therefore exhibit a bloom-and-bust abundance pattern (**Figure 2**)  
333 that might be associated with algal blooms as previous suggested (Kolmonen et al 2004).  
334 On the other hand, bogs also experience seasonal algal blooms (Kent et al 2004, Kent et al  
335 2007) that introduce brief pulses of autochthonous C to these otherwise allochthonous-  
336 driven systems. Clearly, much remains to be learned about the routes through which C is  
337 metabolized by bacteria in such lakes, and comparative genomics is a novel way to use the  
338 organisms to tell us about C flow through the ecosystem.

339

#### 340 **Other genome features of the saccharide-degrading life style**

341 Seven Verrucomicrobia MAGs spanning subdivisions 1, 2, 3, and 4 possess genes needed to  
342 construct bacterial microcompartments (BMCs), which are quite rare among studied  
343 bacterial lineages. Such BMC genes in Planctomycetes are involved in the degradation of  
344 plant and algal cell wall sugars, and are required for growth on L-fucose, L-rhamnose and  
345 fucoidans (Erbilgin et al 2014). Genes involved in L-fucose and L-rhamnose degradation  
346 cluster with BMC shell protein-coding genes in the seven Verrucomicrobia MAGs (**Figure**  
347 **5a**). This is consistent with the high abundance of  $\alpha$ -L-fucosidase or  $\alpha$ -L-rhamnosidase  
348 GH genes in these MAGs (**Figure 4**), suggesting the importance of fucose- and rhamnose-  
349 containing polysaccharides for these Verrucomicrobia populations.

350 TonB-dependent receptor (TBDR) genes were found in Verrucomicrobia MAGs, and  
351 are present at over 20 copies in TE1800 and TH2519. TBDRs are located on the outer  
352 cellular membrane of Gram-negative bacteria, usually mediating the transport of iron  
353 siderophore complex and vitamin B<sub>12</sub> across the outer membrane through an active  
354 process. More recently, TBDRs were suggested to be involved in carbohydrate transport  
355 across the outer membrane by some bacteria that consume complex carbohydrates, and in  
356 their carbohydrate utilization (CUT) loci, TBDR genes usually cluster with genes encoding  
357 inner membrane transporters, GHs and regulators for efficient carbohydrate  
358 transportation and utilization (Blanvillain et al 2007). Such novel CUT loci are present in  
359 TE1800 and TH2519, with TBDR genes clustering with genes encoding inner membrane  
360 sugar transporters, monosaccharide utilization enzymes, and GHs involved in the  
361 degradation of pectin, xylan, and fucose-containing polymers (**Figure 5b**). Notably, most  
362 GHs in the CUT loci are predicted to be extracellular or outer membrane proteins (**Figure**  
363 **5b**), catalyzing extracellular hydrolysis reactions to release mono- and oligo-saccharides,  
364 which are transported across the outer membrane by TBDR proteins. Therefore, such CUT  
365 loci may allow these Verrucomicrobial populations to coordinately and effectively scavenge  
366 the hydrolysis products before they diffuse away.

367 Genes encoding for inner membrane carbohydrate transporters are abundant in  
368 Verrucomicrobia MAGs (**Figure S4**). The Embden-Mayerhof pathway for glucose  
369 degradation, as well as pathways for degrading a variety of other sugar monomers,  
370 including galactose, rhamnose, fucose, xylose, and mannose, were recovered (complete or  
371 partly-complete) in most MAGs (**Figure 6**). As these sugars are abundant carbohydrate  
372 monomers in plankton and plant cell walls, the presence of these pathways together with



373 GH genes suggest that these Verrucomicrobia populations may use plankton- and plant-  
374 derived saccharides. Machinery for pyruvate degradation to acetyl-CoA and the TCA cycle  
375 are also present in most MAGs. These results are largely consistent with their hypothesized  
376 role in carbohydrate degradation and previous studies on Verrucomicrobia isolates.

377 Notably, a large number of genes encoding proteins belonging to a sulfatase family  
378 (pfam00884) are present in the majority of MAGs (**Figure 3b**), similar to the high  
379 representation of these genes in marine Verrucomicrobia genomes (Herlemann et al 2013,  
380 Martinez-Garcia et al 2012a). Sulfatases hydrolyze sulfate esters, which are rich in sulfated  
381 polysaccharides. In general, sulfated polysaccharides are abundant in marine algae and  
382 plants (mainly in seaweeds) (Jiao et al 2011), but have also been found in some freshwater  
383 cyanobacteria (Filali Mouhim et al 1993) and plant species (Dantas-Santos et al 2012).  
384 Sulfatase genes in our Verrucomicrobia MAGs were often located in the same neighborhood  
385 as genes encoding for extracellular proteins with a putative pectin lyase activity, proteins  
386 with a carbohydrate-binding module (pfam13385), GHs, and proteins with PSCyt domains  
387 (**Figure 3c** and discussed later). Their genome context lends support for the participation  
388 of these genes in C and sulfur cycling by degrading sulfated polysaccharides, which can  
389 serve as an abundant source of sulfur for cell biosynthesis as well as C for energy and  
390 growth.

391 Overall, the high abundance of GH, sulfatase, and carbohydrate transporter genes,  
392 metabolic pathways for degrading diverse carbohydrate monomers, and other genome  
393 features adapted to the saccharolytic life style suggest that Verrucomicrobia are primarily  
394 (poly)saccharide-degraders in freshwater, rather than degraders of the algal exudate

395 glycolate as previously suggested (Paver and Kent 2010) (See details of glycolate utilization  
396 by Verrucomicrobia MAGs in **Supplementary Text** and **Figure S5**).

397

### 398 **Nitrogen (N) metabolism and adaptation to different N availabilities**

399 Most Verrucomicrobia MAGs in our study do not appear to reduce nitrate or other  
400 nitrogenous compounds, and they seem to uptake and use ammonia (**Figure 6**), and  
401 occasionally amino acids (**Figure S4**), as an N-source. Further, some Trout Bog populations  
402 may have additional avenues to generate ammonia, including genetic machineries for  
403 assimilatory nitrate reduction in TH2746, nitrogenase genes for nitrogen fixation and  
404 urease genes in some of the Trout Bog MAGs (**Figure 6**), probably as adaptations to N-limited  
405 conditions in Trout Bog.

406         Although Mendota is a eutrophic lake, N can become temporarily limiting during the  
407 high-biomass period when N is consumed by large amounts of phytoplankton and  
408 bacterioplankton (Beverdorsdorf et al 2013). For some bacteria, when N is temporarily  
409 limited while C is in excess, cells convert and store the extra C as biopolymers. For example,  
410 the verrucomicrobial methanotroph *M. fumariolicum* SoIV accumulated a large amount of  
411 glycogen (up to 36% of the total dry weight of cells) when the culture was N-limited  
412 (Khadem et al 2012). Similar to this verrucomicrobial methanotroph, genes in glycogen  
413 biosynthesis are present in most MAGs from Mendota and Trout Bog (**Figure 6**). Indeed, a  
414 glycogen synthesis pathway is also present in most Verrucomicrobia genomes in the public  
415 database (data not shown), suggesting that glycogen accumulation might be a common  
416 feature for this phylum to cope with the changing pools of C and N in the environment and  
417 facilitate their survival when either is temporally limited.

418 To cope with long-term sustained N-limitation, such as that which occurs in Trout  
419 Bog, some bacteria may have evolved features to minimize N cost in amino acid and  
420 nucleotide biosynthesis, thus having reduced proteome N-contents and low genome G+C  
421 contents (Bragg and Hyder 2004, Grzymiski and Dussaq 2012). Grzymiski and Dussaq  
422 (2012) used the numbers of N and C atoms per amino-acid residue side chain (ARSC) for  
423 each predicted protein to indicate proteome N-contents. Based on ARSC, we found that  
424 most, although not all, Trout Bog proteomes have lower N-contents than most Mendota  
425 proteomes, with TE1800, TH2519 and TH4093 having extremely low N-contents (**Figure**  
426 **S6a, c**). Interestingly, proteome C-content is reversely correlated with N-content  
427 (correlation coefficient  $r = -0.83$ ), exhibiting an opposite trend in terms of N and C atom  
428 usage between the two lakes (**Figure S6b, d, e**), probably reflecting the extremely high  
429 DOC and low available N in Trout Bog as compared to Mendota. The genome G+C contents  
430 ranged from 42% to 68%, and are positively correlated to proteome N-contents ( $r = 0.84$ )  
431 (**Figure S6f**), consistent with the expectation that low G+C genomes are favored under  
432 long-term N limitation (Bragg and Hyder 2004). Therefore, genome G+C and proteome N  
433 contents both suggest that some of the Verrucomicrobia populations in Trout Bog have  
434 been adapted to long-term N-limitation.

435

### 436 **Phosphorus (P) metabolism and other metabolic features**

437 Verrucomicrobia populations represented by these MAGs may be able to survive under low  
438 P conditions, as suggested by the presence of genes responding to P limitation, such as the  
439 two-component regulator (*phoRB*), alkaline phosphatase (*phoA*), phosphonoacetate  
440 hydrolase (*phnA*), and high-affinity phosphate-specific transporter system (*pstABC*)

441 **(Figure 6)**. Detailed discussion in P acquisition and metabolism and other metabolic  
442 aspects, such as acetate metabolism, sulfur metabolism, oxygen tolerance, and the presence  
443 of the alternative complex III and cytochrome *c* oxidase genes in the oxidative  
444 phosphorylation pathway, are discussed in the Supplementary Text **(Figure S7)**.

445

#### 446 **Anaerobic respiration and a putative porin-multiheme cytochrome *c* system**

447 Respiration using alternative electron acceptors is important for overall lake metabolism in  
448 the DOC-rich humic Trout Bog, as the oxygen levels decrease quickly with depth in the  
449 water column. We therefore searched for genes involved in anaerobic respiration, and  
450 found that genes in the dissimilatory reduction of nitrate, nitrite, sulfate, sulfite, DMSO, and  
451 TMAO are largely absent in all MAGs **(Supplementary Text, Figure S7)**. Compared to  
452 those anaerobic processes, genes for dissimilatory metal reduction are less well  
453 understood. In more extensively studied cultured iron [Fe(III)] reducers, outer surface *c*-  
454 type cytochromes (*cytc*), such as OmcE and OmcS in *Geobacter sulfurreducens* are involved  
455 in Fe(III) reduction at the cell outer surface (Mehta et al 2005). Further, a periplasmic  
456 multiheme cytochrome *c* (MHC, e.g. MtrA in *Shewanella oneidensis* and OmaB/OmaC in *G.*  
457 *sulfurreducens*) can be embedded into a porin (e.g. MtrB in *S. oneidensis* and OmbB/OmbC  
458 in *G. sulfurreducens*), forming a porin-MHC complex as an extracellular electron transfer  
459 (EET) conduit to reduce extracellular Fe(III) (Liu et al 2014, Shi et al 2014). Such outer  
460 surface *cytc* and porin-MHC systems involved in Fe(III) reduction were also suggested to be  
461 important in reducing the quinone groups in humic substances (HS) at the cell surface  
462 (Bucking et al 2012, Shyu et al 2002, Voordeckers et al 2010). The reduced HS can be re-  
463 oxidized by Fe(III) or oxygen, thus HS can serve as electron shuttles to facilitate Fe(III)

464 reduction (Lovley et al 1996, Lovley and Blunt-Harris 1999) or as regenerateable electron  
465 acceptors at the anoxic-oxic interface or over redox cycles (Klupfel et al 2014).

466 Outer surface *cytc* or porin-MHC systems homologous to the ones in *G.*  
467 *sulfurreducens* and *S. oneidensis* are not present in Verrucomicrobia MAGs. Instead, we  
468 identified a novel porin-coding gene clustering with MHC genes in six MAGs (**Figure 5c**).  
469 These porins were predicted to have at least 20 transmembrane motifs, and their adjacent  
470 *cytc* were predicted to be periplasmic proteins with eight conserved heme-binding sites. In  
471 several cases, a gene encoding an extracellular MHC is also located in the same gene cluster.  
472 As their gene organization is analogous to the porin-MHC gene clusters in *G. sulfurreducens*  
473 and *S. oneidensis*, we hypothesize that these genes in Verrucomicrobia may encode a novel  
474 porin-MHC complex involved in EET.

475 As these porin-MHC gene clusters are novel, we further confirmed that they are  
476 indeed from Verrucomicrobia. Their containing contigs were indeed classified to  
477 Verrucomicrobia based on the consensus of the best BLASTP hits for genes on these  
478 contigs. Notably, the porin-MHC gene cluster was only observed in MAGs recovered from  
479 the HS-rich Trout Bog, especially from the anoxic hypolimnion environment. Searching the  
480 NCBI and IMG databases for the porin-MHC gene clusters homologous to those in Trout  
481 Bog, we identified homologs in genomes within the Verrucomicrobia phylum, including  
482 *Opitutus terrae* PB90-1 isolated from rice paddy soil, *Opitutus* sp. GAS368 isolated from  
483 forest soil, “*Candidatus Udaeobacter copiosus*” recovered from prairie soil, *Opititae*-40 and  
484 *Opititae*-129 recovered from freshwater sediment, and Verrucomicrobia bacterium  
485 IMCC26134 recovered from freshwater; some of their residing environments are also rich  
486 in HS. Therefore, based on the occurrence pattern of porin-MHC among Verrucomicrobia

487 genomes, we hypothesize that such porin-MHCs might participate in EET to HS in anoxic  
488 HS-rich environments, and HS may further shuttle electrons to poorly soluble metal oxides  
489 or be regenerated at the anoxic-oxic interface, thereby diverting more C flux to respiration  
490 instead of fermentation and methanogenesis, which could impact the overall energy  
491 metabolism and green-house gas emission in the bog environment.

492

### 493 **Occurrence of Planctomycete-specific cytochrome *c* and domains**

494 One of the interesting features of Verrucomicrobia and its sister phyla in the PVC  
495 superphylum is the presence of a number of novel protein domains in some of their  
496 member genomes (Kamneva et al 2012, Studholme et al 2004). These domains were  
497 initially identified in marine planctomycete *Rhodopirellula baltica* (Studholme et al 2004)  
498 and therefore, were referred to as “Planctomycete-specific”, although some of them were  
499 later identified in other PVC members (Kamneva et al 2012). In our Verrucomicrobia MAGs,  
500 most genes containing Planctomycete-specific cytochrome *c* domains (PSCyt1 to PSCyt3)  
501 also contain other Planctomycete-specific domains (PSD1 through PSD5) with various  
502 combinations and arrangements (**Figure 7** and **S8a**). Further, PSCyt2-containing and  
503 PSCyt3-containing genes are usually next to two different families of unknown genes,  
504 respectively (**Figure S8b**). Such conserved domain architectures and gene organizations, as  
505 well as their high occurrence frequencies in some of the Verrucomicrobia MAGs are  
506 intriguing, yet nothing is known about their functions. However, some of the PSCyt-  
507 containing genes also contain protein domains identifiable as carbohydrate-binding  
508 modules (CBMs), suggesting a role in carbohydrate metabolism (see detailed discussion in  
509 **Supplementary Text**).

510           The coding density of PSCyt-containing genes indicates that they tend to be more  
511 abundant in the epilimnion (either ME or TE) genomes (**Figure 3c**) and exhibit a reverse  
512 correlation with the GH coding density ( $r = -0.62$ ). Interestingly, sulfatase-coding genes are  
513 often in the neighborhood of PSCyt-containing genes in ME and TE genomes, whereas  
514 sulfatase-coding genes often neighbor with GH genes in TH genomes. The genomic context  
515 suggests PSCyt-containing gene functions somewhat mirror those of GHs (although their  
516 reaction mechanisms likely differ fundamentally). However, these PSCyt-containing genes  
517 were predicted to be periplasmic or cytoplasmic proteins rather than extracellular or outer  
518 membrane proteins. Hence, if they are indeed involved in carbohydrate degradation, they  
519 likely act on mono- or oligomers that can be transported into the cell. Further, the  
520 distribution patterns of GH versus PSCyt-containing genes between the epilimnion and  
521 hypolimnion may reflect the difference in oxygen availability and their carbohydrate  
522 substrate complexity between the two layers, suggesting some niche differentiation within  
523 Verrucomicrobia in freshwater systems. Therefore, a plausible hypothesis is that these  
524 bacterial populations have evolved different genetic machineries to use carbohydrates of  
525 different complexities under different oxygen and C availabilities.

526

## 527 **SUMMARY**

528 Verrucomicrobia MAGs recovered from the two contrasting lakes greatly expanded the  
529 known genomic diversity of freshwater Verrucomicrobia, revealed the ecophysiology and  
530 some interesting adaptive features of this ubiquitous yet less understood freshwater  
531 lineage. The overrepresentation of GH, sulfatase, and carbohydrate transporter genes, the  
532 genetic potential to use various sugars, and the microcompartments for fucose and

533 rhamnose degradation suggest that they are primarily (poly)saccharide degraders in  
534 freshwater. Most of the MAGs encode machineries to cope with the changing availability of  
535 N and P and can survive nutrient limitation. Despite these generalities, these  
536 Verrucomicrobia differ significantly between lakes in the abundance and functional profiles  
537 of their GH genes, which may reflect different C sources of the two lakes. Further, several  
538 Trout Bog MAGs exhibit N cost minimization in their proteomes and genomes, likely an  
539 adaptation to long-term sustained N limitation. Interestingly, a number of MAGs in Trout  
540 Bog possess gene clusters potentially encoding a novel porin-multiheme cytochrome *c*  
541 complex, and might be involved in extracellular electron transfer in the anoxic humic-rich  
542 environment. Intriguingly, large numbers of Planctomycete-specific cytochrome *c*-  
543 containing genes are present in MAGs from the epilimnion, exhibiting nearly opposite  
544 distribution patterns with GH genes. Future studies are needed to elucidate the functions of  
545 these novel and fascinating genomic features.

546

#### 547 **CONFLICT OF INTEREST**

548 The authors declare no conflict of interest.

549

#### 550 **ACKNOWLEDGEMENTS**

551 We thank the North Temperate Lakes Microbial Observatory 2007-2012 field crews, UW-  
552 Trout Lake Station, the UW Center for Limnology, and the Global Lakes Ecological  
553 Observatory Network for field and logistical support. We give special thanks to past  
554 McMahan lab graduate students Ashley Shade, Ryan Newton, Emily Read, and Lucas  
555 Beversdorf. We acknowledge efforts by many McMahan Lab undergrads and technicians



556 related to sample collection and DNA extraction, particularly Georgia Wolfe. KDM  
557 acknowledges funding from the United States National Science Foundation Microbial  
558 Observatories program (MCB-0702395), the Long Term Ecological Research program  
559 (NTL-LTER DEB-1440297) and an INSPIRE award (DEB-1344254). This material is also  
560 based upon work that supported by the National Institute of Food and Agriculture, U.S.  
561 Department of Agriculture (Hatch Project 1002996). Finally, we personally thank the  
562 individual program directors and leadership at the National Science Foundation for their  
563 commitment to continued support of long term ecological research.

564

565

## 566 **REFERENCE**

567 Albertsen M, Hugenholtz P, Skarshewski A, Nielsen KL, Tyson GW, Nielsen PH (2013).  
568 Genome sequences of rare, uncultured bacteria obtained by differential coverage binning of  
569 multiple metagenomes. *Nat Biotech* 31: 533-538.

570

571 Arnds J, Knittel K, Buck U, Winkel M, Amann R (2010). Development of a 16S rRNA-targeted  
572 probe set for Verrucomicrobia and its application for fluorescence in situ hybridization in a  
573 humic lake. *Systematic and applied microbiology* 33: 139-148.

574

575 Bagos PG, Liakopoulos TD, Spyropoulos IC, Hamodrakas SJ (2004). PRED-TMBB: a web  
576 server for predicting the topology of beta-barrel outer membrane proteins. *Nucleic Acids*  
577 *Res* 32: W400-404.

578

579 Bendall ML, Stevens SLR, Chan L-K, Malfatti S, Schwientek P, Tremblay J, Schackwitz W,  
580 Martin J, Pati A, Bushnell B, Froula J, Kang D, Tringe SG, Bertilsson S, Moran MA, Shade A,  
581 Newton RJ, McMahon KD, Malmström RR (2016). Genome-wide selective sweeps and gene-  
582 specific sweeps in natural bacterial populations. *The ISME journal*.

583

584 Beversdorf LJ, Miller TR, McMahon KD (2013). The role of nitrogen fixation in  
585 cyanobacterial bloom toxicity in a temperate, eutrophic lake. *PloS one* 8: e56103.

586

587 Blanvillain S, Meyer D, Boulanger A, Lautier M, Guynet C, Denance N, Vasse J, Lauber E,  
588 Arlat M (2007). Plant carbohydrate scavenging through tonB-dependent receptors: a  
589 feature shared by phytopathogenic and aquatic bacteria. *PloS one* 2: e224.

590

- 591 Bragg JG, Hyder CL (2004). Nitrogen versus carbon use in prokaryotic genomes and  
592 proteomes. *Proceedings Biological sciences / The Royal Society* 271 Suppl 5: S374-377.  
593
- 594 Bucking C, Piepenbrock A, Kappler A, Gescher J (2012). Outer-membrane cytochrome-  
595 independent reduction of extracellular electron acceptors in *Shewanella oneidensis*.  
596 *Microbiology (Reading, England)* 158: 2144-2157.  
597
- 598 Cardman Z, Arnosti C, Durbin A, Ziervogel K, Cox C, Steen AD, Teske A (2014).  
599 *Verrucomicrobia* are candidates for polysaccharide-degrading bacterioplankton in an arctic  
600 fjord of Svalbard. *Applied and environmental microbiology* 80: 3749-3756.  
601
- 602 Chin KJ, Liesack W, Janssen PH (2001). *Opitutus terrae* gen. nov., sp. nov., to accommodate  
603 novel strains of the division 'Verrucomicrobia' isolated from rice paddy soil. *International*  
604 *journal of systematic and evolutionary microbiology* 51: 1965-1968.  
605
- 606 da Rocha UN, van Elsas JD, van Overbeek LS (2010). Real-time PCR detection of *Holophagae*  
607 (*Acidobacteria*) and *Verrucomicrobia* subdivision 1 groups in bulk and leek (*Allium*  
608 *porrum*) rhizosphere soils. *Journal of Microbiological Methods* 83: 141-148.  
609
- 610 Dantas-Santos N, Gomes DL, Costa LS, Cordeiro SL, Costa MS, Trindade ES, Franco CR,  
611 Scortecci KC, Leite EL, Rocha HA (2012). Freshwater plants synthesize sulfated  
612 polysaccharides: heterogalactans from Water Hyacinth (*Eicchornia crassipes*).  
613 *International journal of molecular sciences* 13: 961-976.  
614
- 615 Darling AE, Jospin G, Lowe E, Matsen IV FA, Bik HM, Eisen JA (2014). PhyloSift:  
616 phylogenetic analysis of genomes and metagenomes. *PeerJ* 2: e243.  
617
- 618 Derrien M, Vaughan EE, Plugge CM, de Vos WM (2004). *Akkermansia muciniphila* gen. nov.,  
619 sp. nov., a human intestinal mucin-degrading bacterium. *International journal of systematic*  
620 *and evolutionary microbiology* 54: 1469-1476.  
621
- 622 Edgar RC (2004). MUSCLE: a multiple sequence alignment method with reduced time and  
623 space complexity. *BMC Bioinformatics* 5: 113-113.  
624
- 625 Eiler A, Bertilsson S (2004). Composition of freshwater bacterial communities associated  
626 with cyanobacterial blooms in four Swedish lakes. *Environmental microbiology* 6: 1228-  
627 1243.  
628
- 629 Erbilgin O, McDonald KL, Kerfeld CA (2014). Characterization of a planctomycetal  
630 organelle: a novel bacterial microcompartment for the aerobic degradation of plant  
631 saccharides. *Applied and environmental microbiology* 80: 2193-2205.  
632
- 633 Filali Mouhim R, Cornet J-F, Fontane T, Fournet B, Dubertret G (1993). Production, isolation  
634 and preliminary characterization of the exopolysaccharide of the cyanobacterium *Spirulina*  
635 *platensis*. *Biotechnology Letters* 15: 567-572.  
636

- 637 Freitas S, Hatosy S, Fuhrman JA, Huse SM, Welch DB, Sogin ML, Martiny AC (2012). Global  
638 distribution and diversity of marine Verrucomicrobia. *The ISME journal* 6: 1499-1505.  
639
- 640 Garcia SL, Stevens SLR, Crary B, Martinez-Garcia M, Stepanauskas R, Woyke T, Tringe SG,  
641 Andersson S, Bertilsson S, Malmstrom RR, McMahon KD (2016). Contrasting patterns of  
642 genome-level diversity across distinct co-occurring bacterial populations. *bioRxiv*.  
643
- 644 Grzymski JJ, Dussaq AM (2012). The significance of nitrogen cost minimization in  
645 proteomes of marine microorganisms. *The ISME journal* 6: 71-80.  
646
- 647 Guindon S, Dufayard JF, Lefort V, Anisimova M, Hordijk W, Gascuel O (2010). New  
648 algorithms and methods to estimate maximum-likelihood phylogenies: assessing the  
649 performance of PhyML 3.0. *Systematic biology* 59: 307-321.  
650
- 651 Haukka K, Kolmonen E, Hyder R, Hietala J, Vakkilainen K, Kairesalo T, Haario H, Sivonen K  
652 (2006). Effect of nutrient loading on bacterioplankton community composition in lake  
653 mesocosms. *Microbial ecology* 51: 137-146.  
654
- 655 Hedlund BP, Gosink JJ, Staley JT (1996). Phylogeny of Prostheco bacter, the fusiform  
656 caulobacters: members of a recently discovered division of the bacteria. *International  
657 journal of systematic bacteriology* 46: 960-966.  
658
- 659 Hedlund BP, Gosink JJ, Staley JT (1997). Verrucomicrobia div. nov., a new division of the  
660 bacteria containing three new species of Prostheco bacter. *Antonie van Leeuwenhoek* 72:  
661 29-38.  
662
- 663 Herlemann DP, Lundin D, Labrenz M, Jurgens K, Zheng Z, Aspeborg H, Andersson AF  
664 (2013). Metagenomic de novo assembly of an aquatic representative of the  
665 verrucomicrobial class Spartobacteria. *mBio* 4: e00569-00512.  
666
- 667 Hugerth L, Larsson J, Alneberg J, Lindh M, Legrand C, Pinhassi J, Andersson A (2015).  
668 Metagenome-assembled genomes uncover a global brackish microbiome. *Genome Biology*  
669 16: 279.  
670
- 671 Jiao G, Yu G, Zhang J, Ewart HS (2011). Chemical structures and bioactivities of sulfated  
672 polysaccharides from marine algae. *Marine drugs* 9: 196-223.  
673
- 674 Kamneva OK, Knight SJ, Liberles DA, Ward NL (2012). Analysis of genome content  
675 evolution in pvc bacterial super-phylum: assessment of candidate genes associated with  
676 cellular organization and lifestyle. *Genome biology and evolution* 4: 1375-1390.  
677
- 678 Kang DD, Froula J, Egan R, Wang Z (2015). MetaBAT, an efficient tool for accurately  
679 reconstructing single genomes from complex microbial communities. *PeerJ* 3: e1165.  
680

- 681 Kent AD, Jones SE, Yannarell AC, Graham JM, Lauster GH, Kratz TK, Triplett EW (2004).  
682 Annual Patterns in Bacterioplankton Community Variability in a Humic Lake. *Microbial*  
683 *ecology* 48: 550-560.
- 684  
685 Kent AD, Yannarell AC, Rusak JA, Triplett EW, McMahon KD (2007). Synchrony in aquatic  
686 microbial community dynamics. *The ISME journal* 1: 38-47.
- 687  
688 Khadem AF, van Teeseling MC, van Niftrik L, Jetten MS, Op den Camp HJ, Pol A (2012).  
689 Genomic and Physiological Analysis of Carbon Storage in the Verrucomicrobial  
690 Methanotroph "Ca. Methylophilum Fumariolicum" SolV. *Frontiers in microbiology* 3:  
691 345.
- 692  
693 Klupfel L, Piepenbrock A, Kappler A, Sander M (2014). Humic substances as fully  
694 regenerable electron acceptors in recurrently anoxic environments. *Nature Geosci* 7: 195-  
695 200.
- 696  
697 Kolmonen E, Sivonen K, Rapala J, Haukka K (2004). Diversity of cyanobacteria and  
698 heterotrophic bacteria in cyanobacterial blooms in Lake Joutikas, Finland. *Aquatic*  
699 *Microbial Ecology* 36: 201-211.
- 700  
701 Lindström ES, Vrede K, Leskinen E (2004). Response of a member of the Verrucomicrobia,  
702 among the dominating bacteria in a hypolimnion, to increased phosphorus availability.  
703 *Journal of Plankton Research* 26: 241-246.
- 704  
705 Lindström ES, Kamst-Van Agterveld MP, Zwart G (2005). Distribution of Typical  
706 Freshwater Bacterial Groups Is Associated with pH, Temperature, and Lake Water  
707 Retention Time. *Applied and environmental microbiology* 71: 8201-8206.
- 708  
709 Liu Y, Wang Z, Liu J, Levar C, Edwards MJ, Babauta JT, Kennedy DW, Shi Z, Beyenal H, Bond  
710 DR, Clarke TA, Butt JN, Richardson DJ, Rosso KM, Zachara JM, Fredrickson JK, Shi L (2014).  
711 A trans-outer membrane porin-cytochrome protein complex for extracellular electron  
712 transfer by *Geobacter sulfurreducens* PCA. *Environmental Microbiology Reports* 6: 776-  
713 785.
- 714  
715 Lovley DR, Coates JD, Blunt-Harris EL, Phillips EJP, Woodward JC (1996). Humic substances  
716 as electron acceptors for microbial respiration. *Nature* 382: 445-448.
- 717  
718 Lovley DR, Blunt-Harris EL (1999). Role of humic-bound iron as an electron transfer agent  
719 in dissimilatory Fe(III) reduction. *Applied and environmental microbiology* 65: 4252-4254.
- 720  
721 Markowitz VM, Chen I-MA, Palaniappan K, Chu K, Szeto E, Pillay M, Ratner A, Huang J,  
722 Woyke T, Huntemann M, Anderson I, Billis K, Varghese N, Mavromatis K, Pati A, Ivanova  
723 NN, Kyrpides NC (2013). IMG 4 version of the integrated microbial genomes comparative  
724 analysis system. *Nucleic Acids Research*.
- 725

- 726 Martinez-Garcia M, Brazel DM, Swan BK, Arnosti C, Chain PS, Reitenga KG, Xie G, Poulton NJ,  
727 Lluesma Gomez M, Masland DE, Thompson B, Bellows WK, Ziervogel K, Lo CC, Ahmed S,  
728 Gleasner CD, Detter CJ, Stepanauskas R (2012a). Capturing single cell genomes of active  
729 polysaccharide degraders: an unexpected contribution of Verrucomicrobia. *PloS one* 7:  
730 e35314.  
731
- 732 Martinez-Garcia M, Swan BK, Poulton NJ, Gomez ML, Masland D, Sieracki ME, Stepanauskas  
733 R (2012b). High-throughput single-cell sequencing identifies photoheterotrophs and  
734 chemoautotrophs in freshwater bacterioplankton. *The ISME journal* 6: 113-123.  
735
- 736 Mehta T, Coppi MV, Childers SE, Lovley DR (2005). Outer membrane c-type cytochromes  
737 required for Fe(III) and Mn(IV) oxide reduction in *Geobacter sulfurreducens*. *Applied and*  
738 *environmental microbiology* 71: 8634-8641.  
739
- 740 Newton RJ, Jones SE, Eiler A, McMahon KD, Bertilsson S (2011). A Guide to the Natural  
741 History of Freshwater Lake Bacteria. *Microbiology and Molecular Biology Reviews* : MMBR  
742 75: 14-49.  
743
- 744 Otsuka S, Suenaga T, Vu HT, Ueda H, Yokota A, Senoo K (2013a). *Brevifollis gellanilyticus*  
745 *gen. nov., sp. nov., a gellan-gum-degrading bacterium of the phylum Verrucomicrobia.*  
746 *International journal of systematic and evolutionary microbiology* 63: 3075-3078.  
747
- 748 Otsuka S, Ueda H, Suenaga T, Uchino Y, Hamada M, Yokota A, Senoo K (2013b).  
749 *Roseimicrobium gellanilyticum gen. nov., sp. nov., a new member of the class*  
750 *Verrucomicrobiae.* *International journal of systematic and evolutionary microbiology* 63:  
751 1982-1986.  
752
- 753 Parveen B, Mary I, Vellet A, Ravet V, Debroas D (2013). Temporal dynamics and  
754 phylogenetic diversity of free-living and particle-associated Verrucomicrobia communities  
755 in relation to environmental variables in a mesotrophic lake. *FEMS microbiology ecology*  
756 83: 189-201.  
757
- 758 Paver SF, Kent AD (2010). Temporal patterns in glycolate-utilizing bacterial community  
759 composition correlate with phytoplankton population dynamics in humic lakes. *Microbial*  
760 *ecology* 60: 406-418.  
761
- 762 Pol A, Heijmans K, Harhangi HR, Tedesco D, Jetten MS, Op den Camp HJ (2007).  
763 Methanotrophy below pH 1 by a new Verrucomicrobia species. *Nature* 450: 874-878.  
764
- 765 Qiu YL, Kuang XZ, Shi XS, Yuan XZ, Guo RB (2014). *Terrimicrobium sacchariphilum gen.*  
766 *nov., sp. nov., an anaerobic bacterium of the class 'Spartobacteria' in the phylum*  
767 *Verrucomicrobia, isolated from a rice paddy field.* *International journal of systematic and*  
768 *evolutionary microbiology* 64: 1718-1723.  
769
- 770 Read JS, Rose KC (2013). Physical responses of small temperate lakes to variation in  
771 dissolved organic carbon concentrations. *Limnology and Oceanography* 58: 921-931.

- 772  
773 Sangwan P, Chen X, Hugenholtz P, Janssen PH (2004). *Chthoniobacter flavus* gen. nov., sp.  
774 nov., the first pure-culture representative of subdivision two, Spartobacteria classis nov., of  
775 the phylum Verrucomicrobia. *Applied and environmental microbiology* 70: 5875-5881.  
776
- 777 Sangwan P, Kovac S, Davis KE, Sait M, Janssen PH (2005). Detection and cultivation of soil  
778 verrucomicrobia. *Applied and environmental microbiology* 71: 8402-8410.  
779
- 780 Scheuermayer M, Gulder TA, Bringmann G, Hentschel U (2006). *Rubritalea marina* gen.  
781 nov., sp. nov., a marine representative of the phylum 'Verrucomicrobia', isolated from a  
782 sponge (Porifera). *International journal of systematic and evolutionary microbiology* 56:  
783 2119-2124.  
784
- 785 Schlesner H (1987). *Verrucomicrobium spinosum* gen. nov., sp. nov.: a fimbriated  
786 prosthecate bacterium. *Systematic and applied microbiology* 10: 54-56.  
787
- 788 Schlesner H, Jenkins C, Staley J (2006). The Phylum Verrucomicrobia: A Phylogenetically  
789 Heterogeneous Bacterial Group. In: Dworkin M, Falkow S, Rosenberg E, Schleifer K-H,  
790 Stackebrandt E (eds). *The Prokaryotes*. Springer New York. pp 881-896.  
791
- 792 Shade A, Jones SE, McMahon KD (2008). The influence of habitat heterogeneity on  
793 freshwater bacterial community composition and dynamics. *Environmental microbiology*  
794 10: 1057-1067.  
795
- 796 Shi L, Fredrickson JK, Zachara JM (2014). Genomic analyses of bacterial porin-cytochrome  
797 gene clusters. *Frontiers in microbiology* 5: 657.  
798
- 799 Shieh WY, Jean WD (1998). *Alterococcus agarolyticus*, gen.nov., sp.nov., a halophilic  
800 thermophilic bacterium capable of agar degradation. *Canadian journal of microbiology* 44:  
801 637-645.  
802
- 803 Shyu JBH, Lies DP, Newman DK (2002). Protective Role of *tolC* in Efflux of the Electron  
804 Shuttle Anthraquinone-2,6-Disulfonate. *Journal of bacteriology* 184: 1806-1810.  
805
- 806 Spring S, Bunk B, Sproer C, Schumann P, Rohde M, Tindall BJ, Klenk HP (2016).  
807 Characterization of the first cultured representative of Verrucomicrobia subdivision 5  
808 indicates the proposal of a novel phylum. *The ISME journal* 10: 2801-2816.  
809
- 810 Studholme DJ, Fuerst JA, Bateman A (2004). Novel protein domains and motifs in the  
811 marine planctomycete *Rhodopirellula baltica*. *FEMS microbiology letters* 236: 333-340.  
812
- 813 Voordeckers JW, Kim BC, Izallalen M, Lovley DR (2010). Role of *Geobacter sulfurreducens*  
814 outer surface c-type cytochromes in reduction of soil humic acid and anthraquinone-2,6-  
815 disulfonate. *Applied and environmental microbiology* 76: 2371-2375.  
816

- 817 Wertz JT, Kim E, Breznak JA, Schmidt TM, Rodrigues JLM (2012). Genomic and  
818 Physiological Characterization of the Verrucomicrobia Isolate *Diplosphaera colitermitum*  
819 gen. nov., sp. nov., Reveals Microaerophily and Nitrogen Fixation Genes. *Applied and*  
820 *environmental microbiology* 78: 1544-1555.  
821
- 822 Yin Y, Mao X, Yang J, Chen X, Mao F, Xu Y (2012). dbCAN: a web resource for automated  
823 carbohydrate-active enzyme annotation. *Nucleic Acids Res* 40: W445-451.  
824
- 825 Yoon J, Yasumoto-Hirose M, Katsuta A, Sekiguchi H, Matsuda S, Kasai H, Yokota A (2007).  
826 *Coralimargarita akajimensis* gen. nov., sp. nov., a novel member of the phylum  
827 'Verrucomicrobia' isolated from seawater in Japan. *International journal of systematic and*  
828 *evolutionary microbiology* 57: 959-963.  
829
- 830 Yoon J, Matsuo Y, Katsuta A, Jang JH, Matsuda S, Adachi K, Kasai H, Yokota A (2008).  
831 *Haloferula rosea* gen. nov., sp. nov., *Haloferula harenae* sp. nov., *Haloferula phyci* sp. nov.,  
832 *Haloferula helveola* sp. nov. and *Haloferula sargassicola* sp. nov., five marine  
833 representatives of the family Verrucomicrobiaceae within the phylum 'Verrucomicrobia'.  
834 *International journal of systematic and evolutionary microbiology* 58: 2491-2500.  
835
- 836 Yu CS, Chen YC, Lu CH, Hwang JK (2006). Prediction of protein subcellular localization.  
837 *Proteins* 64: 643-651.  
838
- 839 Yu NY, Wagner JR, Laird MR, Melli G, Rey S, Lo R, Dao P, Sahinalp SC, Ester M, Foster LJ,  
840 Brinkman FSL (2010). PSORTb 3.0: improved protein subcellular localization prediction  
841 with refined localization subcategories and predictive capabilities for all prokaryotes.  
842 *Bioinformatics* 26: 1608-1615.  
843
- 844 Zwart G, Huismans R, van Agterveld MP, Van de Peer Y, De Rijk P, Eenhoorn H, Muyzer G,  
845 van Hannen EJ, Gons HJ, Laanbroek HJ (1998). Divergent members of the bacterial division  
846 Verrucomicrobiales in a temperate freshwater lake. *FEMS microbiology ecology* 25: 159-  
847 169.  
848
- 849 Zwart G, van Hannen EJ, Kamst-van Agterveld MP, Van der Gucht K, Lindström ES, Van  
850 Wichelen J, Lauridsen T, Crump BC, Han S-K, Declerck S (2003). Rapid Screening for  
851 Freshwater Bacterial Groups by Using Reverse Line Blot Hybridization. *Applied and*  
852 *environmental microbiology* 69: 5875-5883.  
853  
854

855 **TABLES**

856

**Table 1. Lakes included in this study<sup>a</sup>**

Lake	Mendota	Trout Bog
GPS location	43.100°N, 89.405°W	46.041°N, 89.686°W
Lake type	Drainage lake	Seepage lake
Surface area (ha)	3938	1.1
Mean depth (m)	12.8	5.6
Max depth (m)	25.3	7.9
pH	8.3	5.2
Primary carbon source	Phytoplankton	Terrestrial subsidies
DOC (mg/L)	5.6	19.9
Total N (mg/L)	1.5	1.3
Total P (µg/L)	131	71
DOC/N	3.7	15.5
DOC/P	42.6	281.0
Trophic state	Eutrophic	Dystrophic

857 <sup>a</sup>Data from NTL-LTER <https://lter.limnology.wisc.edu>, averaged from the study years. DOC = Dissolved  
858 organic carbon. N = Nitrogen. P = Phosphorus.

859

860

861

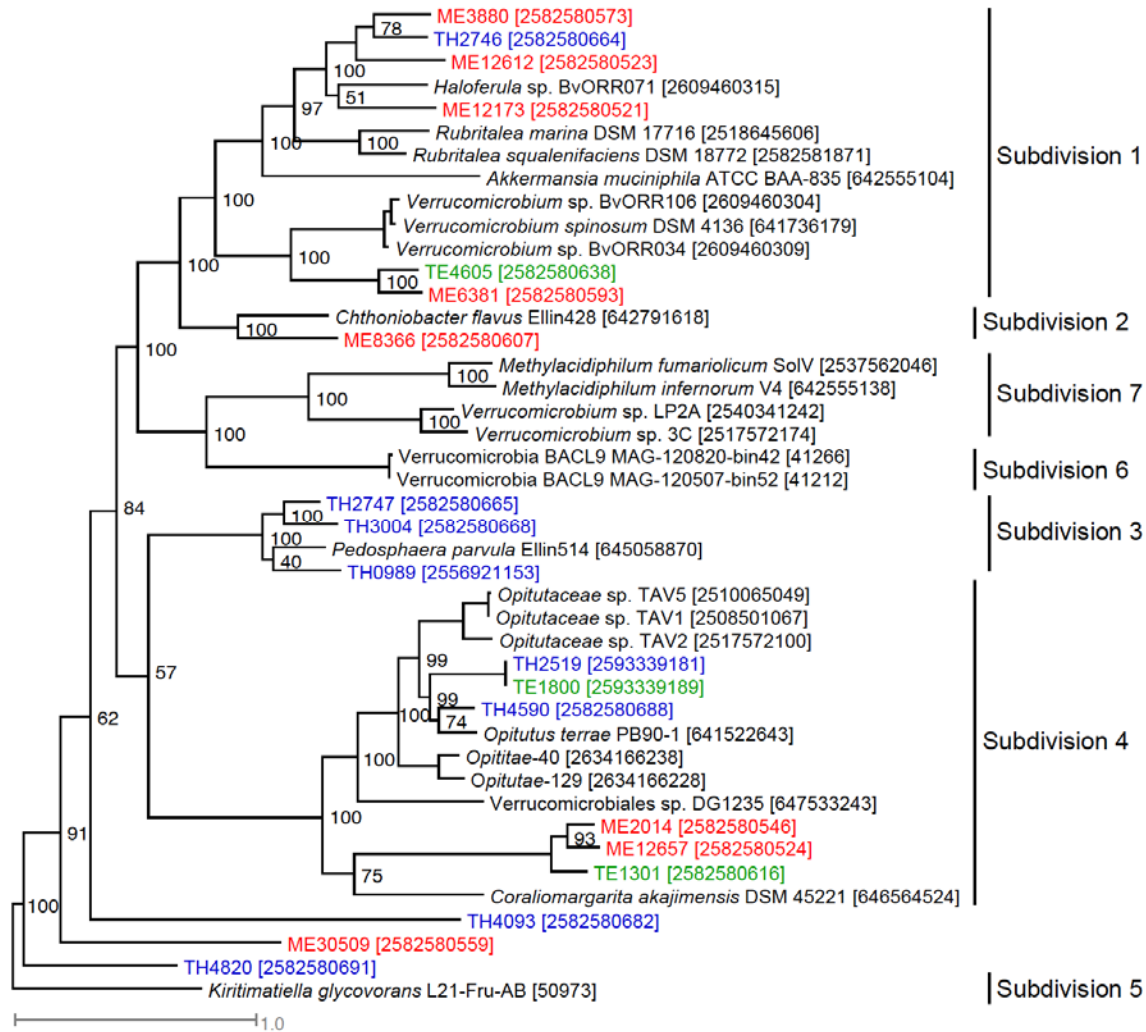
**Table 2. Characteristics of Verrucomicrobia MAGs**

Genome	IMG Taxon OID	Subdivision	Genome Completeness (%)	Recovered Genome Size (Mbp)	GC content (%)	Coding Base (%)	Gene Count
ME3880	2582580573	1	76	1.6	58	90.89	1585
TH2746	2582580664	1	87	6.5	62	86.67	5430
ME12612	2582580523	1	88	2.2	59	88.98	2335
ME12173	2582580521	1	56	2.1	52	91.29	2070
TE4605	2582580638	1	89	4.7	59	91.07	4380
ME6381	2582580593	1	68	2.4	57	92.45	2221
ME8366	2582580607	2	74	3.6	63	87.36	3450
TH2747	2582580665	3	89	5.2	58	89.64	4846
TH3004	2582580668	3	88	4.5	57	91.37	3798
TH0989	2556921153	3	95	7.2	62	90.33	5583
TH2519	2593339181	4	84	1.8	42	94.34	1654
TE1800	2593339189	4	92	2.2	42	94.29	1998
TH4590	2582580688	4	92	3.3	65	90.73	3132
ME2014	2582580546	4	53	1.9	66	93.72	1700
ME12657	2582580524	4	82	1.9	68	94.01	1838
TE1301	2582580616	4	96	2.0	54	94.74	1943
TH4093	2582580682	Unclassified	70	4.7	48	86.52	3982
ME30509	2582580559	Unclassified	78	1.2	63	92.25	1160
TH4820	2582580691	Unclassified	64	3.0	63	86.71	2794

862



863 **FIGURES**  
864



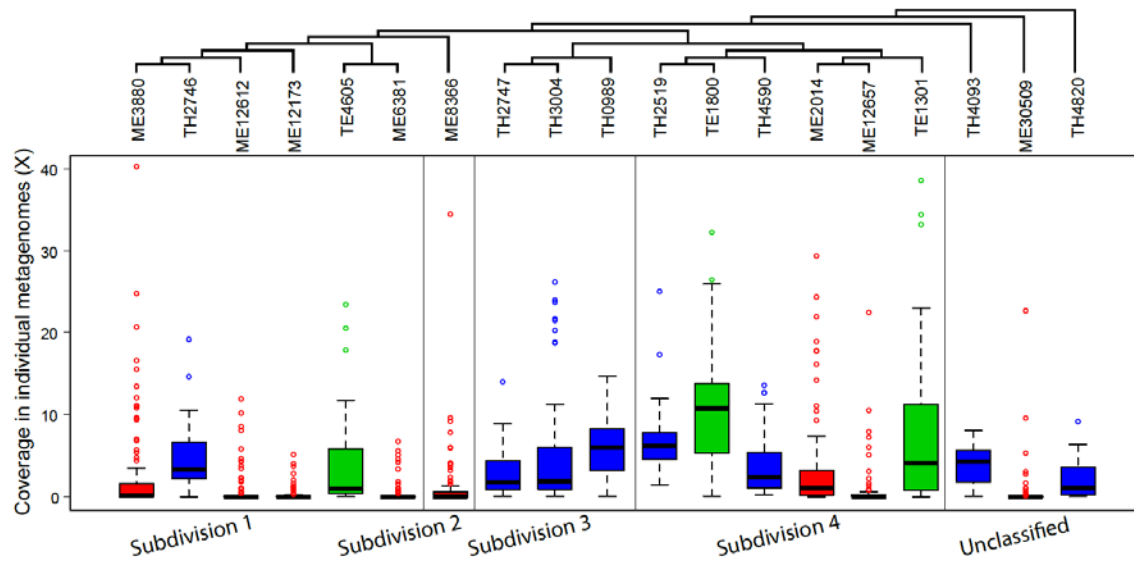
865

866

867 **Figure 1.** Phylogenetic tree constructed with a concatenated alignment of protein  
868 sequences from five conserved essential single-copy genes, which were found in all MAGs.  
869 ME, TE and TH MAGs are labeled with red, green and blue, respectively. Genome ID in IMG  
870 or NCBI is indicated in the bracket. The outgroup is *Kiritimatiella glycovorans* L21-Fru-AB,  
871 which was initially assigned to subdivision 5, but this subdivision was recently proposed as  
872 a novel sister phylum to *Verrucomicrobia* (Spring et al 2016).

873

874



875

876

877 **Figure 2.** A boxplot showing the fold coverage of the 19 MAGs in individual metagenomes.

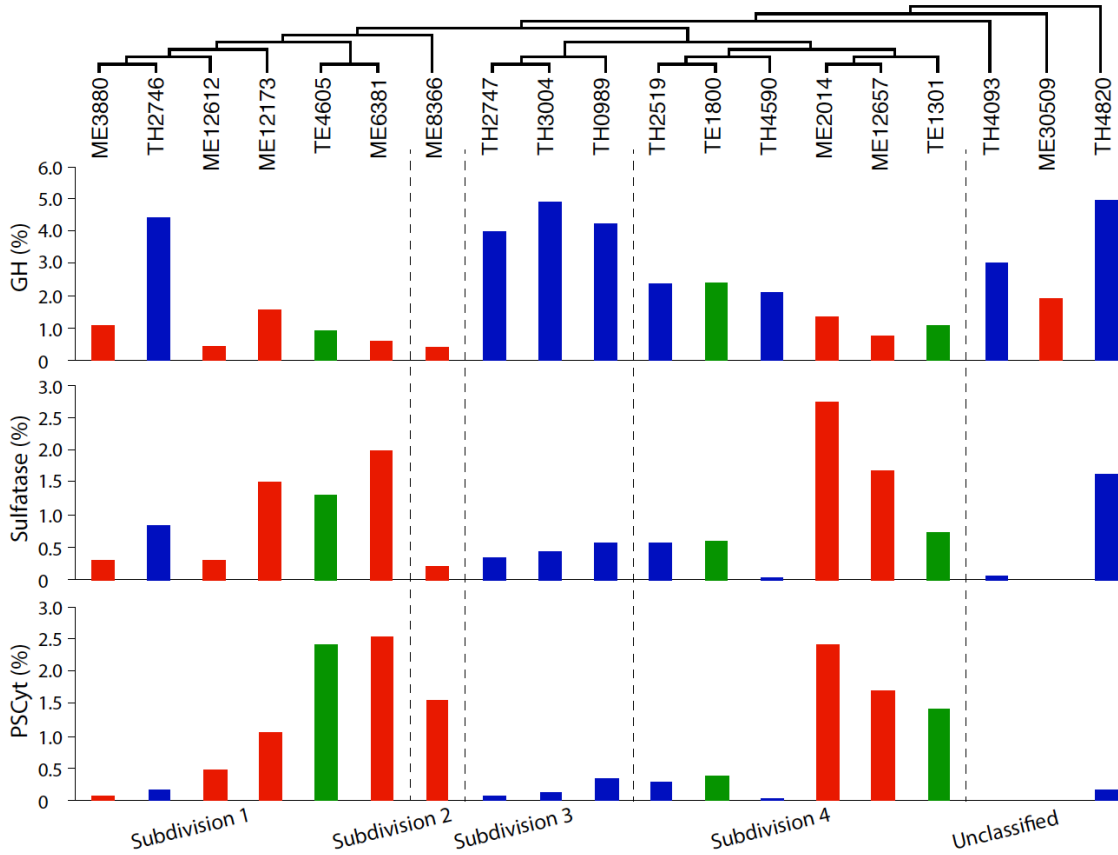
878 The boxplot whiskers are defined by 1.5 times the interquartile range above the upper

879 quartile and below the lower quartile, respectively. ME, TE and TH MAGs are labeled with

880 red, green and blue, respectively. Genome clustering on the top is based on a subtree

881 extracted from the phylogenetic tree in Figure 1 to indicate the phylogenetic relatedness of

882 the 19 MAGs.



883

884

885 **Figure 3.** Coding densities of glycoside hydrolase genes (a), sulfatase genes (b) and  
886 Planctomycete-specific cytochrome *c* (PSCyt)-containing genes (c). Data from ME, TE and  
887 TH MAGs are labeled with red, green and blue, respectively.

888

889

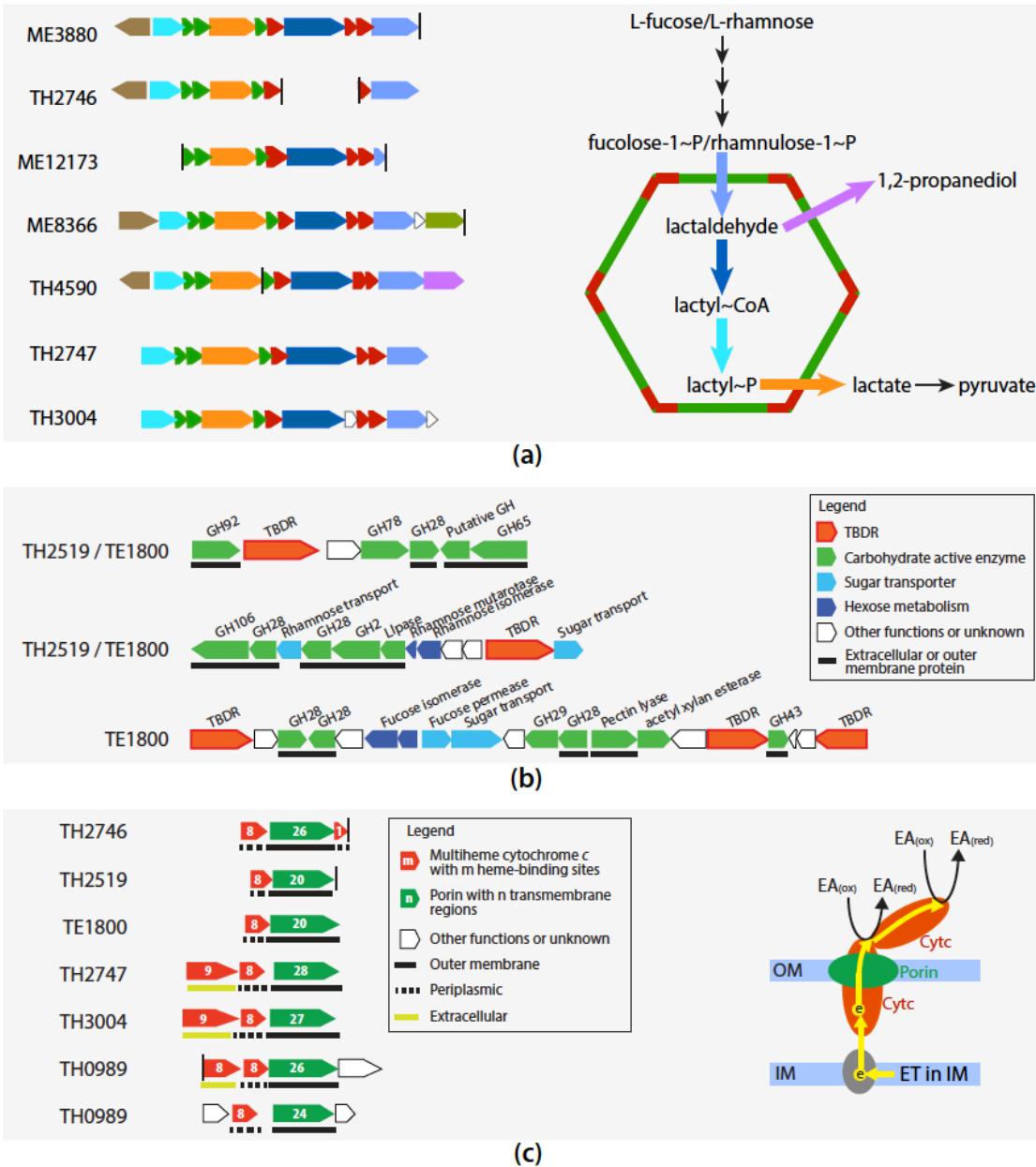
890

GH families	Main Activities																				
		ME3880	TH2746	ME12612	ME12173	TE4605	ME6381	ME8366	TH2747	TH3004	TH0989	TH2519	TE1800	TH4590	ME2014	ME12657	TE1301	TH4093	ME30509	TH4820	
GH29	$\alpha$ -fucosidases	2	22	0	1	0	0	0	17	19	24	4	5	6	0	0	0	14	3	13	
GH2	$\beta$ -galactosidases and other $\beta$ -linked dimers	1	24	0	1	2	0	0	18	14	20	5	5	5	0	0	0	6	2	7	
GH78	$\alpha$ -L-rhamnosidases	1	31	0	2	0	0	0	11	11	13	3	5	9	0	0	0	5	2	7	
GH95	1,2- $\alpha$ -L-fucosidase	0	29	0	1	0	0	0	7	9	17	1	2	3	0	0	0	4	0	7	
GH106	$\alpha$ -L-rhamnosidase	0	21	1	0	0	0	0	4	9	12	1	2	1	0	0	0	3	1	10	
GH13	$\alpha$ -amylase	3	3	2	2	3	2	1	7	6	7	2	3	2	2	2	2	3	0	3	
GH20	$\beta$ -hexosaminidase	0	14	0	4	0	0	0	3	5	2	2	2	3	1	2	4	10	1	3	
GH5	endoglucanase, endomannanase, $\beta$ -glucosidase, $\beta$ -mannosidase	0	4	0	1	4	1	3	13	4	10	0	0	0	0	0	1	6	1	6	
GH28	polygalacturonases, related to pectin degradation	0	1	0	0	0	0	0	7	11	2	8	8	3	1	0	1	0	1	3	
GH43	$\alpha$ -L-arabinofuranosidases, endo- $\alpha$ -L-arabinanases, $\beta$ -D-xylosidases	1	4	0	2	2	0	0	11	15	9	1	1	2	0	0	0	0	0	2	
Counts of other GH genes		9	86	7	18	29	10	10	95	83	119	12	15	32	19	10	13	68	11	77	
<b>Total counts of all GH genes</b>		<b>17</b>	<b>239</b>	<b>10</b>	<b>32</b>	<b>40</b>	<b>13</b>	<b>14</b>	<b>193</b>	<b>186</b>	<b>235</b>	<b>39</b>	<b>48</b>	<b>66</b>	<b>23</b>	<b>14</b>	<b>21</b>	<b>119</b>	<b>22</b>	<b>138</b>	
<b>Total number of GH families represented</b>		<b>12</b>	<b>48</b>	<b>7</b>	<b>23</b>	<b>23</b>	<b>7</b>	<b>10</b>	<b>53</b>	<b>49</b>	<b>58</b>	<b>19</b>	<b>21</b>	<b>26</b>	<b>10</b>	<b>10</b>	<b>13</b>	<b>35</b>	<b>15</b>	<b>45</b>	

891

892

893 **Figure 4.** Gene counts for the top 10 most abundant GH families, total gene counts for all  
 894 GH families, and the number of GH families represented by these genes. MAGs are ordered  
 895 as in the clustering in Figure 2.



896

897 **Figure 5.** Gene clusters encoding BMCs involved in L-fucose and L-rhamnose degradation  
 898 (a), putative tonB-dependent carbohydrate utilization (CUT) loci (b), and putative porin-  
 899 multiheme cytochrome *c* complex (c). The vertical line indicates the end of a contig, and  
 900 horizontal lines below genes indicate predicted cellular locations of their encoded proteins.  
 901 In (a), the two building blocks of the BMC and reactions inside the BMC are colored  
 902 according to their encoding genes' color labels on the left side. In (c), putative EET genes  
 903 are shown, and these clusters are in 18.1, 9.0, 6.1, 18.4, 70.0, 10.6 and 10.8 kbp long  
 904 contigs, respectively. In (c), a hypothesized model of extracellular electron transfer is  
 905 shown on the right with yellow arrows indicating electron flows. "ET in IM", electron  
 906 transfer in the inner membrane, "EA<sub>(ox)</sub>" and "EA<sub>(red)</sub>", oxidized and reduced forms of the  
 907 electron acceptor, respectively.

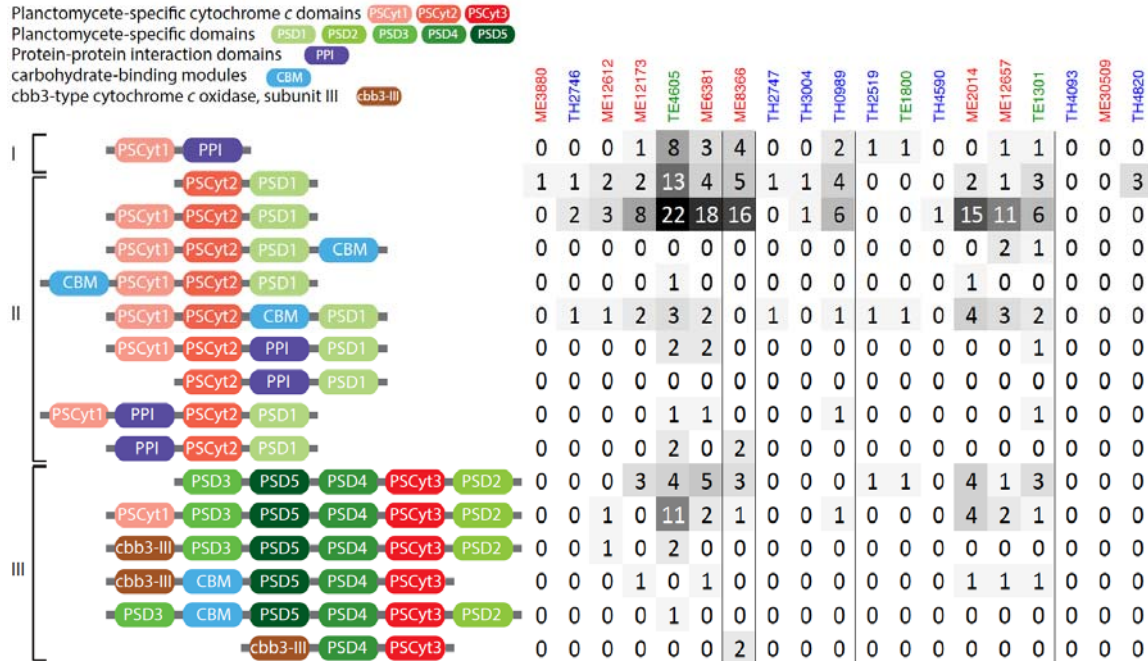
Genes and Pathways	ME3880	TH2746	ME12612	ME12173	TE4605	ME6381	ME8366	TH2747	TH3004	TH0908	TH2519	TE1800	TH4590	ME2014	ME12657	TE1301	TH4093	ME30509	TH4820
<b>Central carbon metabolism</b>																			
Glycolysis (Embden-Meyerhof pathway), glucose => pyruvate	0.78	0.89	0.89	0.67	1	0.89	0.78	1	0.89	1	0.67	0.89	1	0.89	0.56	1	0.89	0.56	0.33
Glycolysis (Entner-Doudoroff pathway)	(0)	(0)	(0)	(0)	(0)	(0)	(0)	(0)	(0)	(0)	(0)	(0)	(0)	(0)	(0)	(0)	(0)	(0)	(0)
Pentose phosphate pathway (Pentose phosphate cycle)	0.86	0.71	0.71	0.71	0.86	0.57	0.71	1	0.86	1	0.71	0.86	1	0.86	0.57	1	0.71	0.29	0.43
Pyruvate oxidation, pyruvate => acetyl-CoA	1	1	1	0	1	1	1	1	1	1	1	1	1	1	1	1	1	1	1
Citrate cycle (TCA cycle, Krebs cycle)	0.63	0.88	1	0.38	0.75	0.63	0.88	0.88	0.88	0.75	1	1	0.88	0.63	0.75	1	0.5	0.25	0.25
<b>Other carbohydrate metabolism</b>																			
Galactose degradation to glycerate-3P	0.5	0.75	0.75	0.25	0.75	0.5	0.5	1	0.75	1	0.5	0.5	0.75	0.25	0.25	0.5	0.75	0.25	0.5
Rhamnose degradation	1	1	0.75	0.5	0.5	0.5	0.5	1	1	1	0.75	1	0.75	0.5	0.5	0.5	1	0.5	0.75
Fucose degradation	1	0.75	0.75	0.25	0.75	0.5	0.75	1	0.75	0.75	0.5	0.75	0.75	0.75	0.5	0.75	1	0.75	0.75
L-Arabinose degradation to xylulose-5P for pentose pathway	1	1	0	0	0.67	0.33	0.33	1	1	1	0	0	0.33	0	0	0	0.67	0.33	0.33
Xylose degradation	1	1	1	1	1	0.5	1	1	1	1	0.5	1	1	1	1	1	0.5	1	1
D-Galacturonate degradation to pyruvate & D-glyceraldehyde 3P	(0)	(0)	(0)	(0)	0.8	0.2	(0)	0.6	(0)	(0)	(0)	(0)	(0)	(0)	(0)	(0)	(0)	(0)	(0)
D-Glucuronate degradation to pyruvate and D-glyceraldehyde 3P	0	0.6	0.4	0.4	0.6	0	0.2	0.6	0.8	0.6	0.6	0.8	0.6	0.2	0.4	0.4	0.6	0.4	0.8
Mannose degradation to glucose-6P	0.5	1	1	1	1	1	1	1	1	1	1	1	1	1	0.5	0.5	1	0.5	1
Lactaldehyde degradation to pyruvate (Aerobic)	1	1	0.33	1	0.33	0.33	1	1	1	0.67	0.33	0.33	1	0.33	0.33	0.33	0.67	0.67	0.67
Glycogen biosynthesis from alpha-D-glucose-6P via ADP-D glucose	0.75	0.25	0.75	0.75	0.75	0.5	1	1	0.75	1	0.5	0.5	1	1	1	1	0.5	0	0.75
<b>Fermentation</b>																			
Pyruvate to acetate via acetyl-coA	1	1	0.67	0.67	0.33	0.33	1	1	1	0.67	0.33	0.33	1	0.67	0.67	0.67	1	1	1
Pyruvate to propanoate	(0)	(0)	(0)	(0)	(0)	(0)	(0)	(0)	(0)	(0)	0.33	0.33	(0)	(0)	(0)	(0)	(0)	(0)	(0)
Pyruvate to succinate	(0)	(0)	(0)	(0)	(0)	(0)	(0)	(0)	(0)	(0)	(0)	(0)	(0)	(0)	(0)	(0)	(0)	(0)	(0)
Pyruvate to butanoate	(0)	(0)	(0)	(0)	(0)	(0)	(0)	(0)	(0)	(0)	(0)	(0)	(0)	(0)	(0)	(0)	(0)	(0)	(0)
Pyruvate to butanol	0.71	0.71	0.71	0.29	1	0.71	0.57	0.43	0.43	0.43	0.57	0.57	1	0.57	0.57	0.57	0.43	0.43	0.43
Pyruvate to ethanol	(0)	(0)	(0)	(0)	(0)	(0)	(0)	(0)	(0)	(0)	(0)	(0)	(0)	(0)	(0)	(0)	(0)	(0)	(0)
Pyruvate to lactate	0	0	0	0	0	0	0	0	0	0	1	1	1	0	0	0	0	0	0
Pyruvate to acetone	(0)	(0)	(0)	(0)	(0)	(0)	(0)	(0)	(0)	(0)	(0)	(0)	(0)	(0)	(0)	(0)	(0)	(0)	(0)
<b>Nitrogen related</b>																			
Dissimilatory nitrate reduction, nitrate => ammonia	0	0	0	0	0	0	0	0	0	0	0	0	(0)	0	0	0	0	0	(0)
Denitrification, nitrate => nitrogen gas	0	0	0	0	0	0	0	0.25	0.25	0	0	0	0	0	0	0	0	0	0
TMAO (trimethylamine-N-oxide) reduction	0	0	0	0	0	0	0	0	0	0	0	0	0	0	0	0	0	0	0
Nitrification, ammonia => nitrite	0	0	0	0	0	0	0	0	0	0	0	0	0	0	0	0	0	0	0
Nitrogen fixation, nitrogen => ammonia	0	0	0	0	0	0	0	1	0	1	0	0	0	0	0	0	1	0	0
Assimilatory nitrate reduction, nitrate => ammonia	0	1	0	0	(0)	0	0	0	0	0	0	0	0	0	0	0	(0)	0	(0)
ABC-type urea transporter	0	0	0	1	0	0	0	0	0	1	0	0	0	0	0	1	0	0	0
Urease (Urea => CO2 + NH3)	0	0	0	0	0	0	0	0	0	1	0	0	1	0	0	1	0	0	0
Ammonia permease	1	1	1	1	1	1	1	1	1	1	0	0	1	0	1	1	1	0	1
<b>Phosphorus related</b>																			
Alkaline phosphatase (PhoA)	1	1	1	1	0	0	1	0	0	0	0	0	0	1	1	1	1	0	0
ABC-type phosphate-specific transport (Pst) system, high-affinity	0	1	1	1	1	1	1	1	1	1	1	1	1	0	1	1	1	1	0
PIT inorganic phosphate transporter (PitA), permease, low-affinity	0	0	0	0	1	1	1	1	1	1	1	1	1	1	1	1	0	0	1
Polyphosphate storage and utilization (PPK)	0	1	1	1	1	1	1	1	1	1	1	1	1	1	1	1	1	1	0
ABC-type phosphonate transport system	0	0	0	0	0	0	0	0	0	0	0	0	0	0	0	0	0	0	0
Phosphonoacetate degradation	0	1	0	1	1	0	1	1	1	0	0	0	1	0	0	0	0	0	0

908

909

910 **Figure 6.** Completeness estimates of key metabolic pathways. MAGs are ordered as in the  
 911 clustering in Figure 2. Completeness value of “1” indicates a pathway is complete; “0”  
 912 indicates no genes were found in that pathway; and “(0)” indicates that although some  
 913 genes in a pathway are present, the pathway is likely absent because signature genes for  
 914 that pathway were not found in that draft genome AND signature genes are missing in  
 915 more than two thirds of all draft genomes.

916



917

918

919 **Figure 7.** Domain architecture and occurrence of PSCyt-containing genes. Based on the  
 920 combination of specific PSCyt and PSD domains, these domain structures can be classified  
 921 into three groups (I, II, and III). “CBM” refers to carbohydrate-binding modules, which  
 922 include pfam13385 (Laminin\_G\_3), pfam08531 (Bac\_rhamnosid\_N), pfam08305 (NPCBM),  
 923 pfam03422 (CBM\_6), and pfam07691 (PA14). “PPI” refers to protein-protein interaction  
 924 domains, which include pfam02368 (Big\_2), pfam00400 (WD40), and pfam00754  
 925 (F5\_F8\_type\_C).

926